A Fan-Equipped Reactor for Dust Explosion Tests

Almerinda Di Benedetto
Dipartimento di Ingegneria Chimica, dei Materiali e della Produzione Industriale, Università degli Studi Federico II, 80125 Napoli, Italy

Paola Russo
Dipartimento di Ingegneria Chimica Materiali Ambiente, Sapienza Università di Roma, 00184 Roma, Italy

Roberto Sanchirico and Valeria Di Sarli
Istituto di Ricerche sulla Combustione - Consiglio Nazionale delle Ricerche (IRC-CNR), 80125 Napoli, Italy

DOI 10.1002/aic.14750
Published online February 23, 2015 in Wiley Online Library (wileyonlinelibrary.com)

A Computational Fluid Dynamics (CFD) model was developed with the aim at simulating the turbulent flow field and associated dust dispersion in an agitated spherical explosion vessel. Simulations were performed in the presence of two counter-rotating fans and also after having switched-off the fans. Numerical results have shown that the dust mainly accumulates at the center of the sphere in the space left by the four vortices formed. After the switch-off of the fans, the dust particles start filling the empty volumes inside the sphere, reaching a quite uniform distribution (with concentration equal to the nominal value) and simultaneously ensuring a controlled value of turbulent kinetic energy. © 2015 American Institute of Chemical Engineers *AIChE J*, 61: 1572–1580, 2015
Keywords: process safety, dust explosion, CFD simulations, 20 L explosion vessel, turbulence, dust dispersion

Introduction

The use of flammable dusts and/or hybrid mixtures (i.e., mixtures of flammable gas/vapor and dust) is increasing in chemical processes (food, pharmaceutical and wood industries, and chemical manufacturing), leading to increased number of accidents imputable to their explosion.

Protection, prevention, and mitigation measures from these accidents require the knowledge of thermo-kinetic parameters that quantify the flammability and explosion features of dust/air and/or dust-gas/air mixtures. Among these parameters, the deflagration index (K_{St}) is very important as it allows the classification of the dust explosion severity.

Measurement of K_{St} is worldwide performed according to a standard procedure as fully described in Ref. 1. The standard explosion apparatus consists of a closed steel combustion chamber with an internal volume of at least 20 L, spherical or cylindrical in shape. As clearly stated in the standard procedure,[2] the vessel must be capable of dispersing a fairly uniform dust cloud of material. Indeed, mal distribution of the dust inside the vessel may modify the flame propagation velocity producing misleading results. Uniformity of the dust concentration in the sphere is of primary importance not only for measurements of the deflagration index (K_{St}) but mainly for measurements of the minimum explosive concentration (MEC).[3]

We have recently shown that the dust/air cloud formed inside the 20 L standard sphere with the rebound nozzle is not uniform.[4–7] In particular, we developed a three-dimensional (3D) CFD model and simulation results have shown that whatever the dust nominal concentration, the dust is mainly concentrated at the boundaries of four vortices formed inside the vessel. At the boundaries of the vortices, the dust concentration is twice the nominal dust concentration. Conversely, at the center of the vessel, where the igniters are positioned, the actual dust concentration is about half the nominal dust concentration. As a result, it may happen that the flame propagation starts at this concentration value, but the MEC estimation corresponds to the value of nominal dust concentration. Based on these findings, novel solutions have to be found.

In the past, Kumar et al.[8] measured the deflagration index and the maximum pressure for different dust concentrations in a 10 m^3 cylindrical vessel in the presence of two fans, one positioned at the top and the other one at the bottom of the vessel. They found that the effect of the turbulence induced by fans is almost negligible on the maximum pressure but substantial on the rate of pressure rise. From these results, it is not possible to derive detailed information about the fluid flow and the dust distribution in the whole vessel.

Here, we present the results of 3D CFD simulations of a novel apparatus in which dust mixing and dispersion are obtained by means of one or two fans positioned at the bottom/top of the spherical 20 L vessel. Numerical results allow to visualize the fluid flow and the dust concentration distribution.

The main aim of the work presented in this article is to demonstrate how a fan-equipped apparatus may allow to overcome the critical issues linked to the actual standard equipment and procedure. It will be shown that the 20 L

Correspondence concerning this article should be addressed to A. Di Benedetto at almerinda.dibenedetto@unina.it.

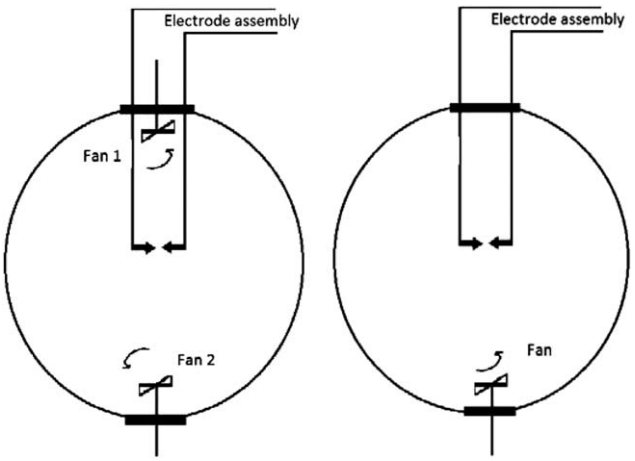

Figure 1. 20 liter explosion vessel with two fans (left) and with one fan (right).

spherical vessel equipped with two fans, positioned one at the top and the other at the bottom, which is under a pending patent,[5] allows a uniform dust distribution to be established inside the sphere with a very low turbulence level when a specific procedure is implemented.

20 L Explosion Vessel with Fans

CFD simulations were run of the 20 L spherical apparatus described in the American Society for Testing and Materials (ASTM) standard E 1226[2]. The major difference is the insertion of one or two fans in substitution of the classic compressed air dispersion system equipped with the rebound nozzle.

Simulations with two fans were performed by assuming the fans as positioned at the bottom and at the top of the sphere (Figure 1 left). In the simulations with one fan, the fan was positioned at the bottom of the sphere (Figure 1 right).

With respect to the standard 20 L equipment, the dust dispersion was not performed with the rebound nozzle but through the fans. It is worth noting that, for this device, also the vacuum and the air feeding lines were eliminated.

Mathematical Model

Computational domain and mesh

The computational domain and mesh were built with the aid of the software Gambit 2.3.16 (www.ansys.com). Figure 2 shows the computational domain of the sphere with the two fans (left) and with one fan (right). The geometrical details of the fan are given in Table 1. The fans were positioned symmetrically with respect to the center of the sphere. The mesh used was unstructured and nonuniform being finer close to the fans. Grid-independent solution was found with total cell number equal to 984267.

Table 1. Geometrical Details of the Fans

Inclination of the blades relative to the xz plane	45°
Number of blades	5
Thickness of the fan (cm)	0.1
Width of the fan (cm)	12.5
Average length of each blade (cm)	3.5

Model equations

To simulate the fans, the two rotating reference frames approach of the ANSYS Fluent code was used.[9] According to this model, individual cell zones can be assigned different rotational and/or translational speeds. The flow in each moving cell zone is solved using the moving reference frame equations. If the zone is stationary, the equations reduce to their stationary forms. At the interfaces between cell zones, a local reference frame transformation is performed to enable flow variables in one zone to be used to calculate fluxes at the boundary of the adjacent zone. In this approach, the mesh remains fixed for the computation.

The frame velocity was assumed as constant and its initial distance from the absolute reference frame is equal to r. The fan walls move with the reference frame around the y axis. The fluid has a relative velocity v_r and a velocity due to the fan rotation (u_r, whirl velocity) calculated as follows

$$\boldsymbol{v}_r = \boldsymbol{v} - \boldsymbol{u}_r \tag{1}$$

$$\boldsymbol{u}_r = \boldsymbol{\omega} \times \boldsymbol{r} \tag{2}$$

where, v is the absolute velocity and ω is the angular velocity of the rotating reference frame with respect to the fixed reference frame.

The continuity equation and the fluid flow momentum balance equation read as follows

$$\nabla \cdot (\rho \boldsymbol{v}_r) = 0 \tag{3}$$

$$\nabla \cdot (\rho \boldsymbol{v}_r \boldsymbol{v}) + \rho(\boldsymbol{\omega} \times \boldsymbol{v}) = -\nabla p + \nabla \cdot \boldsymbol{\tau} + \boldsymbol{F} \tag{4}$$

where $(\boldsymbol{\omega} \times \boldsymbol{v})$ is the centripetal and Coriolis acceleration.

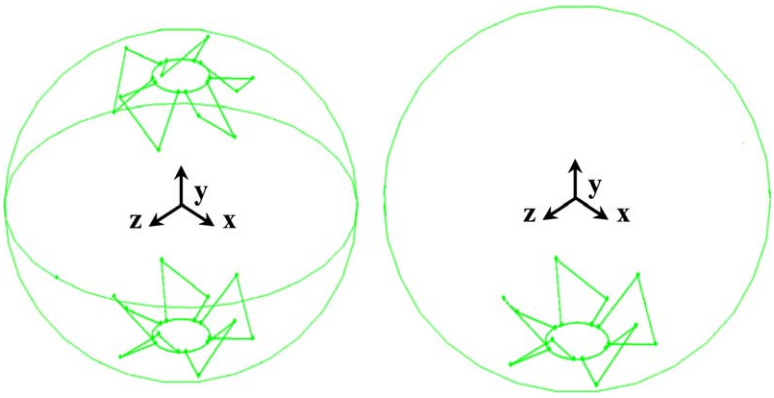

Figure 2. Computational domain of the sphere with the two fans (left) and with one fan (right).

[Color figure can be viewed in the online issue, which is available at wileyonlinelibrary.com.]

Table 2. Setting of the Rotating Reference Frames

Bottom fan	
Origin (x,y,z)	(0,−0.1515,0)
Rotation axis	y
Rotational velocity (rpm)	3000
Top fan	
Origin (x,y,z)	(0,0.1515,0)
Rotation axis	y
Rotational velocity (rpm)	−3000

The turbulence submodel implemented was the $k-\varepsilon$ RNG which includes also the effect of swirl on turbulence

$$\nabla \cdot (\rho \boldsymbol{v} k) = \nabla \cdot (\alpha_k \mu_{\text{eff}} \nabla k) + G_k - \rho\varepsilon \tag{5}$$

$$\nabla \cdot (\rho \boldsymbol{v} \varepsilon) = \nabla \cdot (\alpha_\varepsilon \mu_{\text{eff}} \nabla \varepsilon) + C_{1\varepsilon} \frac{\varepsilon}{k} G_k - C_{2\varepsilon} \rho \frac{\varepsilon^2}{k} \tag{6}$$

where, G_k is the source term of the turbulent kinetic energy due to the gradients of the average velocity, α_k and α_ε are the inverse of the Prandtl numbers for k and ε, constants $C_{1\varepsilon}$ and $C_{2\varepsilon}$ are equal to 1.44 and 1.92, respectively, and μ_{eff} is the turbulence viscosity

$$\mu_{eff} = \mu_0 f\left(\alpha_s, \Omega, \frac{k}{\varepsilon}\right) \tag{7}$$

In Eq. 7, α_s is the swirl constant (assumed as equal to 0.07), Ω is the swirl number and μ_0 is the viscosity evaluated with the following equation

$$\mu_o = \rho C_\mu \frac{k^2}{\varepsilon} \tag{8}$$

with $C_\mu = 0.09$.

The equations of the dust as well as the numerical method adopted have been described in details in our previous article.[4] Briefly, the flow of the solid phase was solved using the discrete phase model (DPM) (Lagrangian approach). The interaction between the fluid phase and the solid particles was modelled by a two-way coupling as suggested by the values of the particle volume fraction, particle density, and particle concentration.[10]

Parallel calculations were performed by means of the segregated pressure-based solver of the ANSYS Fluent code (release 14.0).[11] The pressure-velocity COUPLED method was used to solve the pressure-velocity coupling. To achieve convergence, all residuals were set equal to $1 \cdot \times 10^{-6}$.

Simulation conditions

In Table 2, the conditions adopted for the two rotating reference frames are given. The fan walls are defined as "stationary" with respect to the rotaing reference frame, while the sphere walls are "moving walls" with respect to the rotating reference frame, but with zero velocity with respect to the absolute reference frame. In Table 3, details of the conditions adopted for the fan are given.

The fluid was air at constant atmospheric temperature and pressure. The properties of the dust are given in Table 4.

Table 3. Settings of the Rotating Reference Frame

Origin (x,y,z)	(0,−0.1515,0)
Rotation axis	y
Rotational velocity (rpm)	3000

Table 4. Dust Properties

Density (kg/m^3)	2046
Diameter (μm)	10
Dust concentration (g/m^3)	250

Results and Discussion

Configuration with 1 fan

In Figure 3, the velocity vector map colored by the velocity magnitude is shown as obtained at steady state in the central plane.

Two vortices are shown, arising from the rotation of the fan, mainly located close to the bottom of the sphere, where the fan is positioned. The two vortices are caused by the ascending flow close to the sphere wall and a descending flow close to the sphere axis. The velocity map is steady and its maximum is 18 m/s. In the case of the vessel with the rebound nozzle, the fluid flow decays in time. Initially, the maximum velocity is equal to about 320 m/s and, after 60 m/s (ignition time), the maximum velocity drops to about 14 m/s.[12]

In Figure 4, the map of the turbulent kinetic energy (k) is shown as obtained in the central vertical and horizontal planes of the sphere. The values of k are significantly lower than those obtained in the standard 20 L sphere with the rebound nozzle.[4] Indeed, with the rebound nozzle configuration, we found that after the dust injection, the turbulent kinetic energy reaches peaks as high as 250 m^2/s^2 decaying in time. At the ignition time (t = 60 m/s), the turbulent kinetic energy is about 65 m^2/s^2. In the presence of a fan, the map is steady and the turbulent kinetic energy has much lower values ($k \leq 2.5$ m^2/s^2).

Figure 4 shows that, close to the fan, the maximum values of the kinetic energy are attained at the wall, while far away from the fan, the maximum values of the kinetic energy are attained at the center of the sphere. These results suggest that, in the presence of a fan, the distribution of the kinetic energy is not uniform inside the sphere.

In Figure 5, the path-lines of the dust particles are shown as colored by the particle velocity magnitude. It can be seen

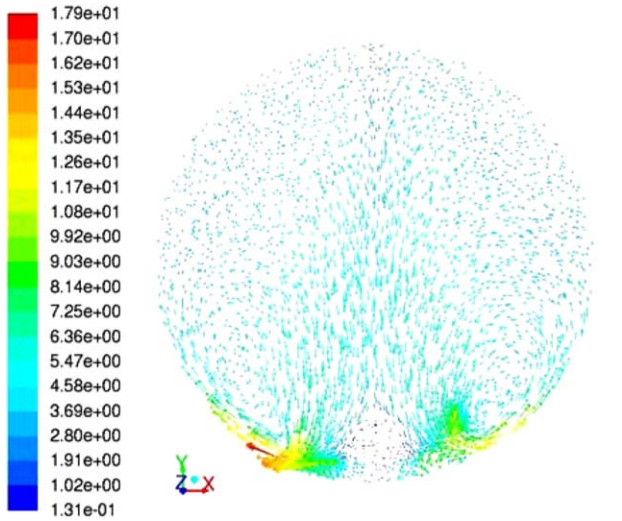

Figure 3. Velocity vectors colored by velocity magnitude (m/s) in the central vertical plane of the sphere.

[Color figure can be viewed in the online issue, which is available at wileyonlinelibrary.com.]

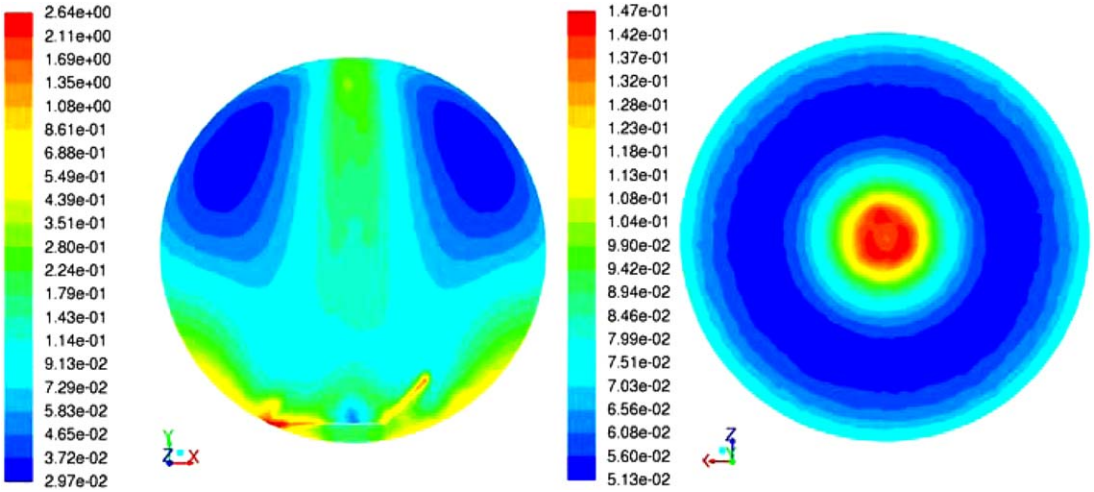

Figure 4. Turbulent kinetic energy (m^2/s^2) maps as computed in the central vertical (left) and central horizontal (right) planes of the sphere.

[Color figure can be viewed in the online issue, which is available at wileyonlinelibrary.com.]

that the dust follows a major helicoidal path close to the vessel walls.

Figure 6 shows the dust particle distribution colored by the dust concentration. It appears that the dust is concentrated at the upper part of the sphere.

In Figure 7, the dust concentration map is shown as computed at the central vertical plane of the sphere. It is found that the dust accumulates at the top of the sphere and at the walls in the upper part of the sphere. The dust does not enter the vortices created by the fan which remain as dead volumes.

From this map, it appears that, at the center of the sphere, the dust presence is almost negligible. As a consequence, if the ignition point is located at the center of the sphere, the explosion parameters and the flammability limit (MEC) are under-estimated.

The dust accumulates at the top of the sphere and at the walls by the motion induced by the fan rotation pushing the dust toward the top and the walls. By comparing the dust distribution inside the sphere with the CFD results obtained in the standard sphere with the rebound nozzle, we may affirm that in both cases the dust is not uniformly dispersed inside the sphere.[4–7] However, in the case of the rebound nozzle, a higher concentration is attained at the center close to the ignition position.

We tested the vessel behavior also after having switched-off the fan. In Figure 8, the dust distribution is shown as colored by the dust concentration (kg/m^3), at different time instances after the fan switch-off (10, 30, and 150 m/s).

From these maps is appears that the dust distribution is quite uniform after 150 m/s in the whole sphere. However, looking at the central plane of the sphere (Figure 9), we notice that the dust is mainly accumulated at the walls at all times.

The maximum dust concentration is found close to the top of the sphere. After the fan switch-off, the dust starts settling on the walls without penetrating into the center of the sphere.

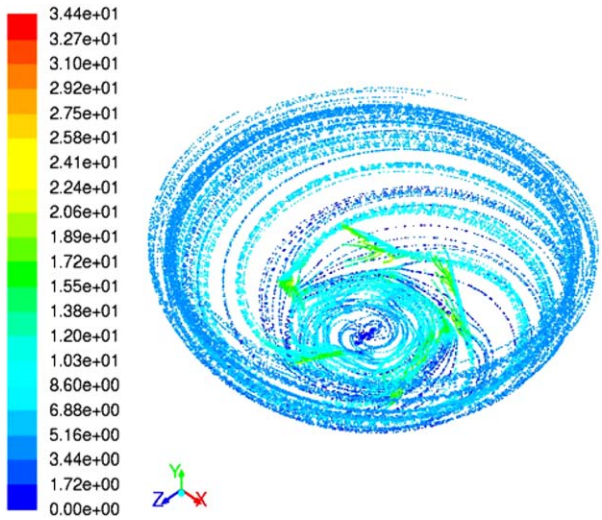

Figure 5. Path-lines of the dust particles colored by the dust velocity magnitude (m/s).

[Color figure can be viewed in the online issue, which is available at wileyonlinelibrary.com.]

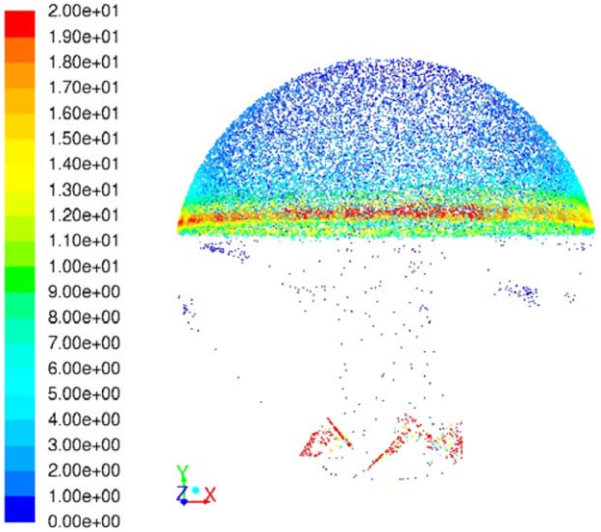

Figure 6. Dust particle distribution colored by dust concentration (kg/m^3).

[Color figure can be viewed in the online issue, which is available at wileyonlinelibrary.com.]

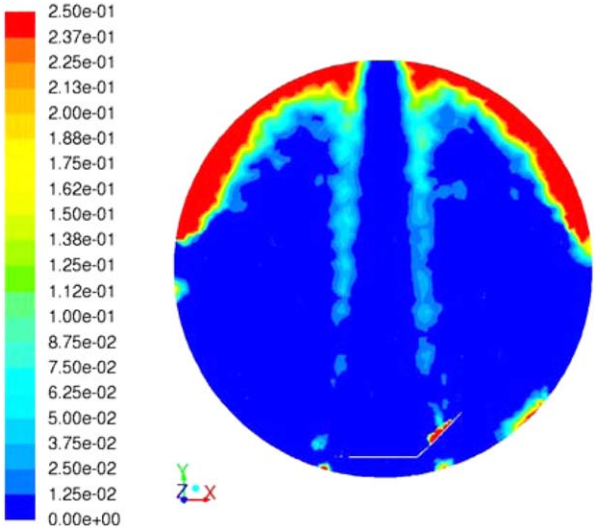

Figure 7. Dust concentration inside the sphere in the central vertical plane (kg/m^3).

[Color figure can be viewed in the online issue, which is available at wileyonlinelibrary.com.]

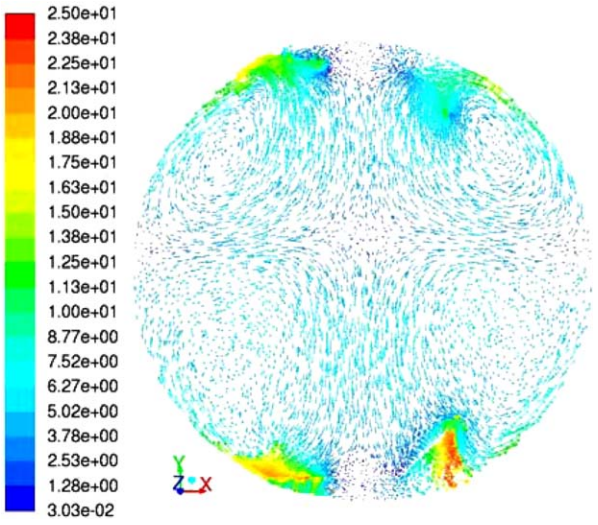

Figure 10. Velocity vectors colored by the velocity magnitude in the central plane of the sphere (m/s).

[Color figure can be viewed in the online issue, which is available at wileyonlinelibrary.com.]

Configuration with 2 fans

In Figure 10, the velocity vectors computed in the whole sphere when using two opposite fans (one at the top and the other one at the bottom) are shown as colored by the velocity magnitude. Four vortices are generated, two located at the top of the sphere and two at the bottom.

In Figure 11, the turbulent kinetic energy is plotted in the central (left) and horizontal (right) plane of the sphere. It

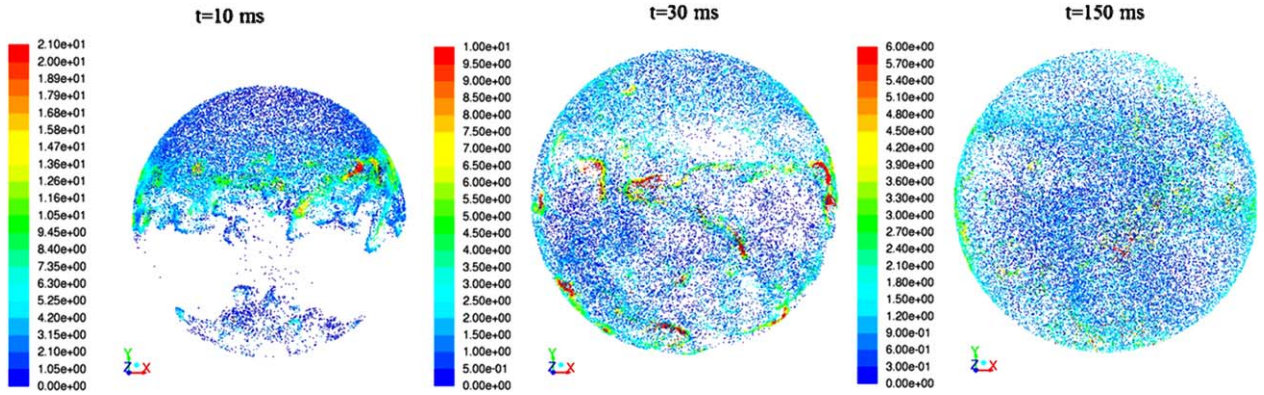

Figure 8. Dust particle distribution colored by dust concentration at different time instances after the fan switch-off (kg/m^3).

[Color figure can be viewed in the online issue, which is available at wileyonlinelibrary.com.]

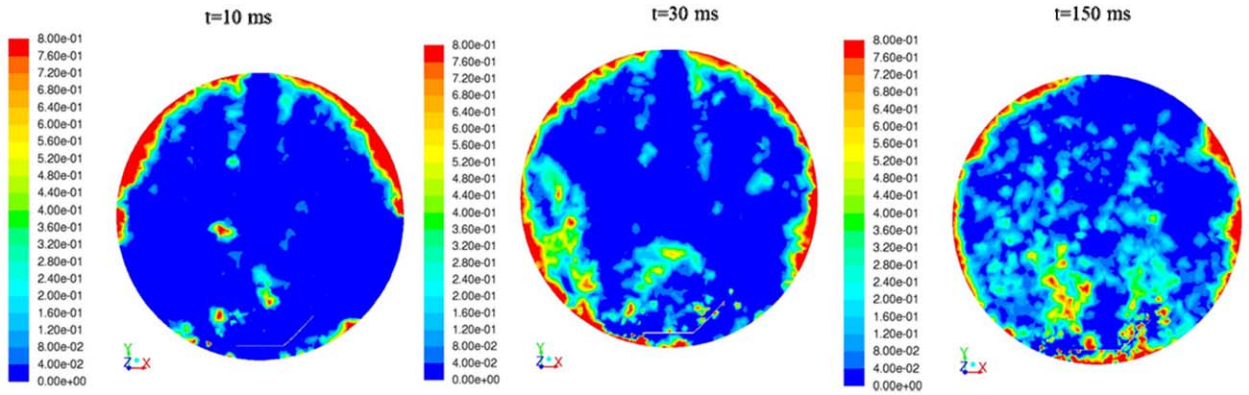

Figure 9. Contour of dust concentration at different time instances after the fan switch-off (central vertical plane) (kg/m^3).

[Color figure can be viewed in the online issue, which is available at wileyonlinelibrary.com.]

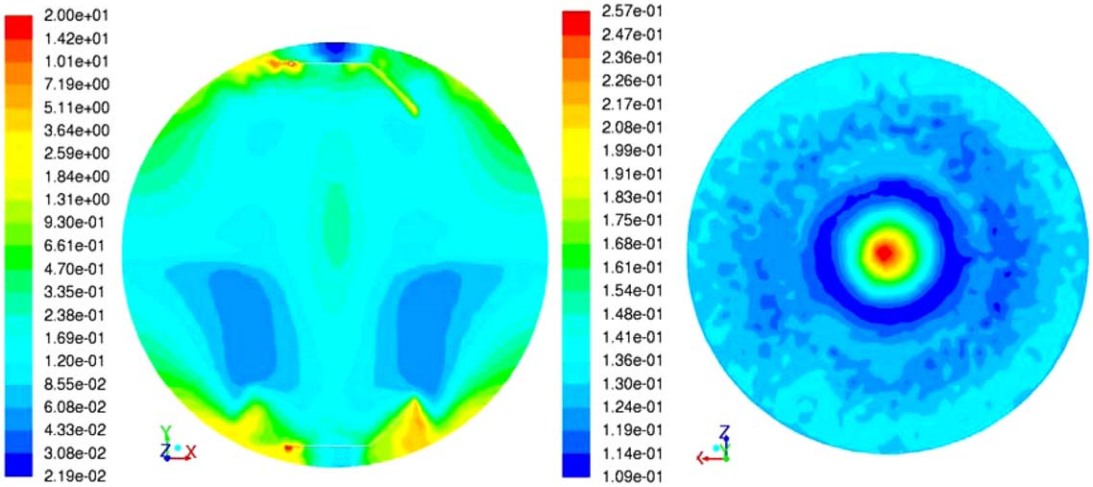

Figure 11. Maps of turbulent kinetic energy in the central (left) and horizontal (right) plane of the sphere (m^2/s^2).

[Color figure can be viewed in the online issue, which is available at wileyonlinelibrary.com.]

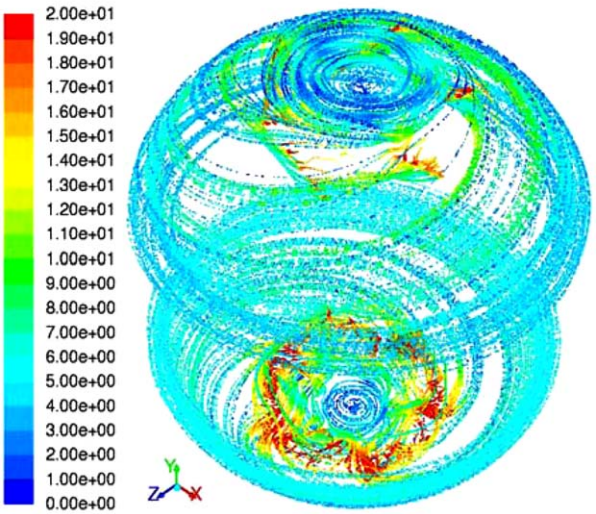

Figure 12. Dust path-lines colored by the dust velocity (m/s).

[Color figure can be viewed in the online issue, which is available at wileyonlinelibrary.com.]

appears that the maximum value of turbulent kinetic energy is reached close to the fans. It is also worth noting that the turbulence level is almost uniform in the most of the sphere.

With respect to the standard sphere with the rebound nozzle, the turbulence level is much lower ($k \sim 1$ m^2/s^2 rather than 30–50 m^2/s^2) and much more uniform.[4,7]

The dust particle path-lines presented in Figure 12 show that the dust is not well dispersed inside the sphere, but it is mainly pushed by the centrifugal force toward the walls of the sphere and it is entrained by the fans themselves following an helicoidal path.

The helicoidal path is clockwise at the top and counterclockwise at the bottom as shown in Figure 13.

The generation of the four vortices inside the sphere causes the presence of dead volumes where the dust cannot enter. Indeed, the dust is concentrated at the boundaries of the vortices (Figure 14).

From these results, it can be concluded that the presence of two counterrotating fans allows the control of the turbulence level (which is uniform), but it does not allow for obtaining a uniform dust cloud.

The nonuniform dust concentration is caused by the presence of centrifugal forces that push the dust at the boundaries

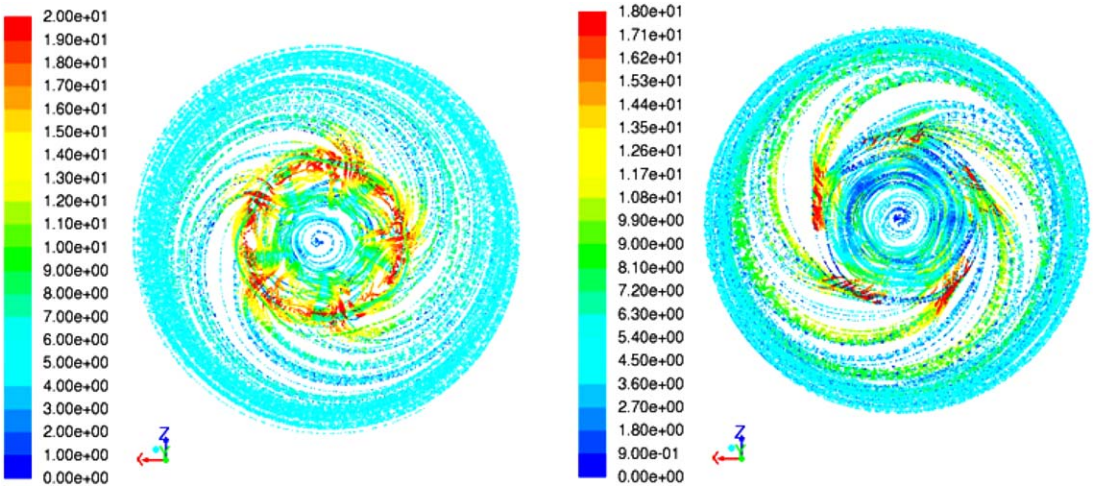

Figure 13. Dust path-lines in the volume close to the bottom (left) and top (right) fan colored by the dust velocity (m/s).

[Color figure can be viewed in the online issue, which is available at wileyonlinelibrary.com.]

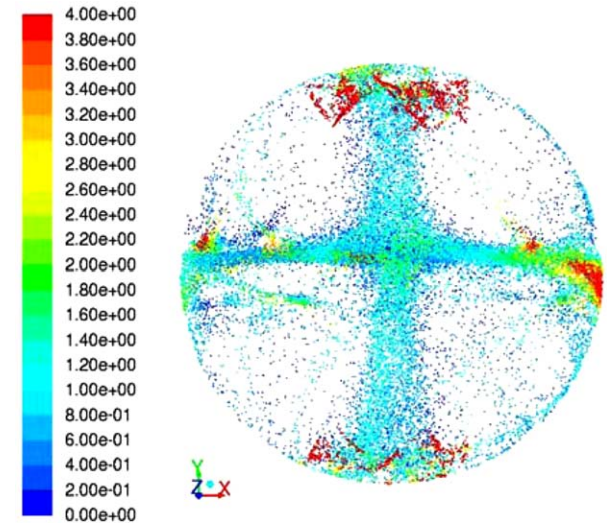

Figure 14. Dust particle distribution colored by dust concentration (kg/m^3).

[Color figure can be viewed in the online issue, which is available at wileyonlinelibrary.com.]

of the vortical structures generated by the fans. In the absence of the centrifugal force, we may expect that the dust is not pushed anymore and it is allowed to enter all the volume of the sphere. We then simulated the temporal evolution of the dust concentration after switching-off the fans.

In Figure 15, the dust distribution (colored by the dust concentration) is shown as computed at different time instances after the fan switch-off ($t = 10$, 50, 100, 150, and 240 m/s).

From the maps of Figure 15, it appears that dust settling starts and rapidly destroys the cross shape distribution ($t = 10$ s), giving rise to a uniform distribution with a concentration equal to the nominal value ($C = 0.25$ kg/m^3) at $t = 240$ m/s.

After the fan switch-off, the dust accumulated at the center of the sphere moves inside the four vortices, which disappear and, thus, are not able to push the dust outside.

After the fan switch-off, the fluid flow and turbulence level start decaying. In Figure 16, the velocity vectors as computed in the central (left) and horizontal (right) plane are shown as colored by the velocity magnitude at $t = 240$ m/s.

The four vortical structures (present with the moving fans) disappear and the velocities decrease reaching an almost uniform value equal to 1 m/s. Also the turbulent kinetic energy (Figure 17) decreases reaching a quite uniform distribution.

These results suggest that the sphere equipped with two fans may be successfully used for generating a uniform dust/air cloud with a controlled and uniform turbulent kinetic energy distribution, provided that a novel procedure is coupled. The novel procedure should be based on the activation of ignition after a delay time from switch-off. According to our simulations, the optimal ignition delay time is equal to 240 m/s.

Chung and Trutt[13] and Chein and Chung[14] modeled particle dispersion in an asymmetric jet. They showed that the extent of particle dispersion depends on the Stokes number ($St = \tau_p/\tau_J$) evaluated as the ratio of particle aerodynamic response time ($\tau_p = \rho\, d_p^2$ /18 μ where ρ is the particles density, d_p is the particle diameter, and μ is the fluid viscosity) to the viscous time scale of the flow ($\tau_J = D/U$ where, D and U are the characteristic diameter and the velocity of the fluid flow).

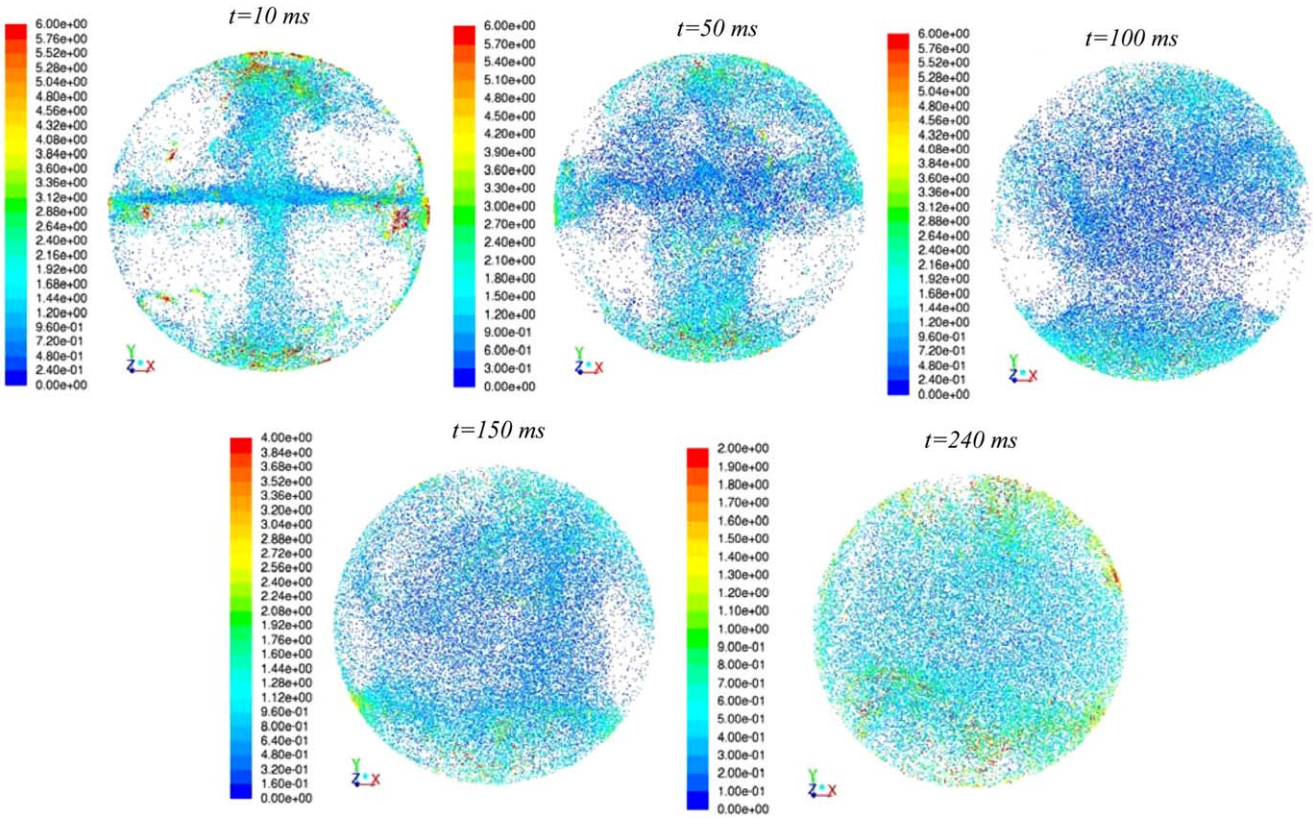

Figure 15. Dust particle distribution colored by dust concentration at different time instances after the fan switch-off (kg/m^3).

[Color figure can be viewed in the online issue, which is available at wileyonlinelibrary.com.]

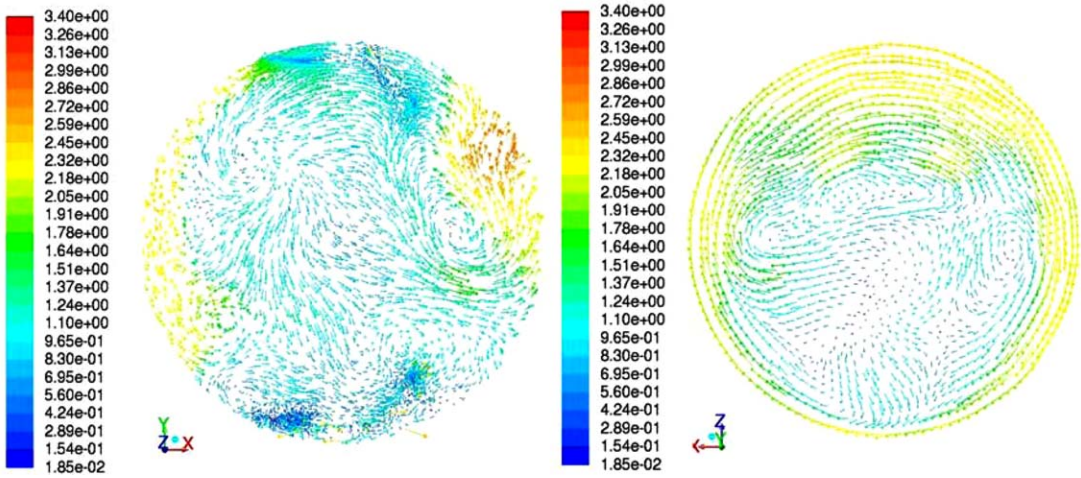

Figure 16. Velocity vectors colored by the velocity magnitude in the central (left) and horizontal (right) plane of the sphere (at $t = 240$ m/s after the fan switch-off) (m/s).

[Color figure can be viewed in the online issue, which is available at wileyonlinelibrary.com.]

Shuen et al.[14] defined a turbulent Stokes number, St_T, as the ratio of the particle relaxation time (τ_p) to the time scale based on a characteristic eddy lifetime (τ_e). τ_e may be evaluated as ($\tau_e = C\ k/\ \varepsilon\ \sqrt{2/3}$) where k and ε are the turbulent kinetic energy and the dissipation rate, respectively and C is a semiempirical coefficient set to 0.09.

We computed both the St and St_T for the two configurations investigated: two fan at steady state and after 240 m/s from two fan switch-off.

We found that in all cases the St and turbulent St_T numbers are lower than 1 (0.01–0.3), suggesting that the particles have sufficient time to respond to the turbulence structure of the fluid flow: the motion of the particles is mainly controlled by the vortex structure of the gas phase. As a consequence, the presence of intense vortical structures as in the configuration with two fans on is not beneficial since the fluid flow itself dictates a particle distribution and entrainment as function of the fluid structure. Accordingly, when the vortices are broken (configuration with fan switched-off) and disappear leading to a much more uniform velocity distribution, the particles are much uniformly dispersed.

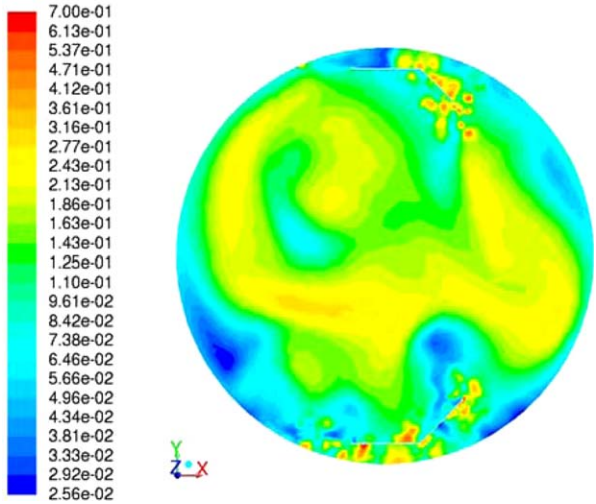

Figure 17. Map of the turbulent kinetic energy in the central plane (at $t = 240$ m/s after the fan switch-off) (m^2/s^2).

[Color figure can be viewed in the online issue, which is available at wileyonlinelibrary.com.]

Conclusions

A 3D CFD model was used to test a novel fan-equipped vessel for flammability and explosion tests. Simulations were performed in the presence of one fan (positioned at the bottom of the vessel) and two counterrotating fans (positioned at the top and at the bottom of the vessel) and also after having switched-off the fan/fans.

Numerical results have shown that, in the presence of only one fan, the dust entrained by the fluid flow mainly accumulates at the top of the sphere. After having switched-off the fan, the dust starts moving along the wall without penetrating into the center of the sphere.

The rotation of two fans guarantees a controlled turbulence level, but it does not allow a uniform dust concentration. In particular, it creates four vortical structures. The dust is centrifuged outside by the vortices, whose internal cores behave as dead volumes for the dust that mainly accumulates at the center of the sphere (in the space left by the vortices formed). After the switch-off of the fans, the dust starts filling the empty volumes inside the sphere, reaching a quite uniform distribution (with concentration equal to the nominal value) and simultaneously ensuring a controlled low value of turbulent kinetic energy.

The results obtained suggest that it is possible to achieve a uniform cloud of dust/air inside the vessel if two fans are used and the novel procedure is implemented. The novel procedure is based on the following steps: (1) steady state with at least two rotating fans; (2) fan switch-off; (3) ignition after a delay time which has been found to be equal to 240 m/s according to our simulations.

In the future, experimental validation of the fluid flow and dust concentration distribution inside the vessel equipped with fans will be performed.

Literature Cited

1. Eckhoff RK. Differences and similarities of gas and dust explosions: a critical evaluation of the European 'ATEX' directives in relation to dusts. *J. Loss Prev Process Ind.* 2006;19:553–560.
2. ASTM E1226. Standard test method for pressure and rate of pressure rise for combustible dusts. In: 2005 ASTM. *Annual Book of*

Standards; American Society for Testing and Materials (ASTM). West Conshohocken, PA: ASTM International, 2005;3–4.
3. ASTM E1515. Standard test method for minimum explosible concentration of combustible dusts. In: 2007 ASTM. *Annual Book of Standards; American Society for Testing and Materials (ASTM)*. West Conshohocken, PA: ASTM International, 2007;2–4.
4. Di Benedetto A, Russo P, Sanchirico R, Di Sarli V. CFD simulations of turbulent fluid flow and dust dispersion in the 20 liter explosion vessel. *AIChE J*. 2013a;59:2485–2496.
5. Di Benedetto A, Bizzarro A, Russo P, Sanchirico R, Di Sarli V. (2013b). Apparatus for the flammability and explosion of dust uniformly dispersed. Italian Patent RM2013A000239, Patent submitted 23/4/2013.
6. Di Sarli V, Russo P, Sanchirico R, Di Benedetto A. CFD simulations of the effect of dust diameter on the dispersion in the 20 l bomb. *Chem Eng Trans*. 2013;31:727–732.
7. Di Sarli V, Russo P, Sanchirico R, Di Benedetto A. CFD simulations of dust dispersion in the 20 L vessel: effect of nominal dust concentration. *J Loss Prev Process Ind*. 2014;27:8–12.
8. Kumar RK, Bowles EM, Mints KJ. Large-scale dust explosion experiments to determine the effects of scaling on explosion parameters. *Combust Flame*. 1992;89:320–332.
9. ANSYS FLUENT User's Guide. ANSYS Fluent Theory Guide, Release 14.0. 2011. Available at www.ansys.com.
10. Elghobashi S. On predicting particle-laden turbulent flows. *Appl Sci Res*. 1994;52:309–329.
11. ANSYS FLUENT. ANSYS Fluent Code, Release 14.0. Available at http://www.ansys.com/Products/Simulation+Technology/Fluid+Dynamics/Fluid+Dynamics+Products/ANSYS+Fluent.
12. Shuen JS, Chen LD, Faeth GM. Evaluation of a stochastic model of particle dispersion in a turbulent round jet. *AIChE J*. 1983;29:167–170.
13. Chung JN and Troutt TR. Simulation of particle dispersion in an axisymmetric jet. *J Fluid Mech*. 1988;186:192–122.
14. Chein R, Chung JN. Simulation of particle dispersion in a two-dimensional mixing layer. *AIChE J*. 1988;34:946–954.

Manuscript received Sep. 12, 2014, and revision received Nov. 28, 2014.